

**Three-dimensional analysis
for the understanding and control**

of the transport phenomena in the Fuel Cell

Yuzoh Yamashita^a, Hisashi Minakuchi^a, Yasunori Okano^a,
Masao Sudoh^a and Sadik Dost^b

^aDepartment of Materials Science & Chemical
Engineering, Shizuoka University,
Johoku 3-5-1, Hamamatsu 432-8561, Japan

^bCrystal Growth Laboratory, University of Victoria,
Victoria, BC, Canada V8W 3P6

A power system based on a fuel cell is a promising alternative to existing energy conversion techniques. Especially, Proton Exchange Membrane Fuel Cell (PEMFC) is expected to be the next generation power sources. However, concentration and temperature distributions in the cell affect the cell performance significantly. Therefore, a precise control of transport phenomena in the system is essential for the development of high performance FC. For the purpose of optimizing a fuel cell structure, a numerical simulation study for the fluid flow, heat and mass transfer occurring in a PEMFC was performed.

The governing equations of the model are three-dimensional continuity, Navier-Stokes, energy and mass transport equations. They were discretized by the finite volume technique on the staggered mesh and solved by the SIMPLE algorithm. The electrochemical reaction at the catalyst layer was considered in the calculation. The schematics of the computational domain are shown in Fig.1. In this analysis, the parallel flow structure is computed. The size and numbers of meshes are shown in Table 1.

Fig.2 shows the ratio of average flux to inlet flux in channel at inlet flux $F_{in} = 1.37 \times 10^{-5} \text{ [m}^3/\text{s]}$. Fig.3 represents the velocity distribution at the depth of $Z=0.5 \text{ [mm]}$. From these figures, it can be seen that the flux in each channel is different. Consequently, this difference in the flux of channels affects the current density distribution as seen in Fig.4. Fig.5 describes vapor concentration distribution in the X-Z plane. Comparison of the channels shows that slower velocity leads to higher vapor concentration. Since the velocity is depended on current density and vapor concentration, the optimization of the flow velocity in each channel is necessary.

Figs.6 and 7 represent the effect of the depth of flow channel on current density at the inlet velocity of $U_{in}=0.452 \text{ [m/s]}$ and the inlet flux of $F_{in} = 1.37 \times 10^{-5} \text{ [m}^3/\text{s]}$, respectively. As shown in Fig. 6, lower depth of channel leads to higher current density. As can be seen in Fig.7, in spite of increased inlet flux, the lowest current density occurs in the case of 1.2 [mm] depth. Therefore, an optimization in terms of channel depth under various

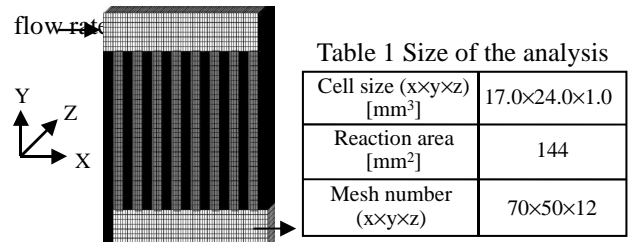


Fig.1 The schematic diagram of the analysis

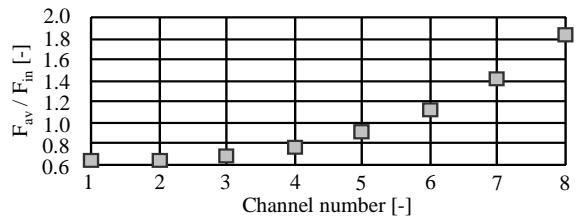


Fig.2 The ratio of average flux to inlet flux in channel flow at inlet flux $F_{in}=1.37 \times 10^{-5} \text{ [m}^3/\text{s]}$

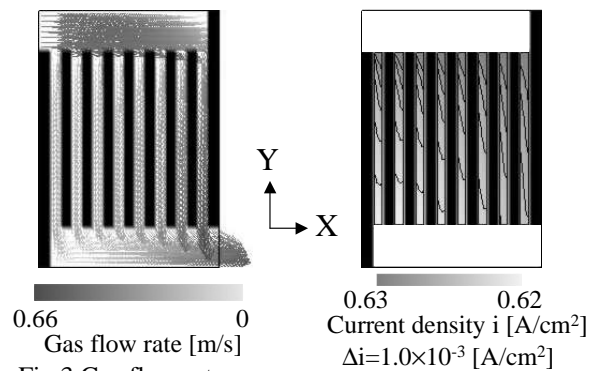


Fig.3 Gas flow rate at $Z=0.5 \text{ [mm]}$

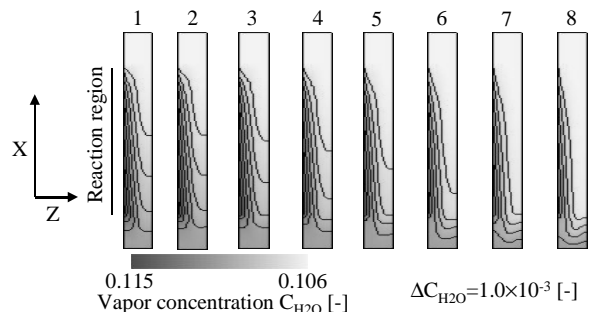


Fig.5 Vapor concentration distribution in each channel

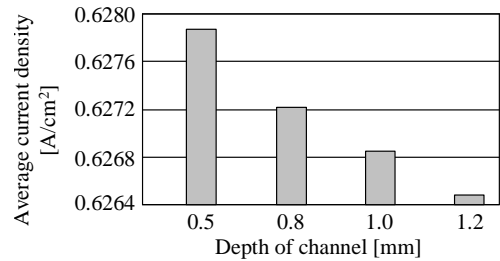


Fig.6 Effect of depth of channel on current density at $U_{in}=0.452 \text{ [m/s]}$

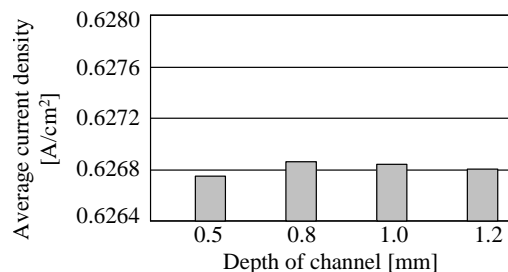


Fig.7 Effect of depth of channel on current density at $1.37 \times 10^{-5} \text{ [m}^3/\text{s]}$